# Statistical ray optics

**Eli Yablonovitch**

*Exxon Research & Engineering Company, P.O. Box 45, Linden, New Jersey 07036*

Received December 17, 1981

A statistical approach is taken toward the ray optics of optical media with complicated nonspherical and nonplanar surface shapes. As a general rule, the light in such a medium will tend to be randomized in direction and of $2n^2(x)$ times greater intensity than the externally incident light, where $n(x)$ is the local index of refraction. A specific method for doing optical calculations in statistical ray optics will be outlined. These optical enhancement effects can result in a new type of antireflection coating. In addition, these effects can improve the efficiency as well as reduce the cost of solar cells.

## 1. INTRODUCTION

Traditionally, geometrical optics has concerned itself with the optical properties of media having spherical and planar surface shapes. Optical materials with more complicated surface shapes, or even with random surface textures, have not been thought to merit any special analytical treatment.

Nevertheless, there are many situations in which the optical properties of materials having complex surface shapes are of paramount importance. For example, in solar cells there is a tendency for light to be trapped by total internal reflection in the semiconductor if at least one of the surfaces is textured.[1–4] In this paper we hope to present a proper analytical approach toward the ray optics of materials with complicated surface shapes.

We adopt a statistical approach that is rather general in that it treats on an equal footing the infinite variety of possible surface shapes and textures. The implicit assumption in such an approach is that the behavior of the light rays is ergodic, i.e., a steady-state, temporally averaged, light-intensity distribution will be identical with a statistical phase-space intensity distribution. Obviously, in some situations the ergodic hypothesis will be invalid and the statistical approach of this paper will not work. We attempt to show how to delineate those nonergodic geometries from the far larger class that can indeed be treated by statistical mechanics.

We find that there is an overriding tendency for the light intensity, internal to an ergodic optical medium, to be $n^2$ times larger than the incident-light intensity. This enhancement can be further multiplied by 2 if the incident illumination is one-sided and a white reflective surface is placed behind the optical medium. In an inhomogeneous medium, the intensity enhancement will be given by the same formula employing the local index of refraction $n(x)$.

In Section 2 we give a derivation based on statistical mechanics. Such an approach is powerful in that it can be generalized to situations in which ray optics is inapplicable (although we will not attempt such a generalization in this article). An effort is made in Section 3 to delineate nonergodic geometries from ergodic geometries. However, we will not attempt to distinguish between these two classes in the mathematically rigorous measure-theory sense.

A geometrical-optics derivation of the intensity enhancement is presented in Section 4. It is a simple example of a useful approach toward optical calculations in statistical ray optics. Its simplicity permits us to recognize better some of the prerequisites and limitations of this type of intensity enhancement. In Section 5 we show how these considerations are modified in the presence of absorption.

Experiments on and analysis of a new type of ray-optics antireflection coating are presented in Section 6. In addition, two types of solar-cell structures are analyzed and the results checked against experiment in Sections 7 and 8.

## 2. STATISTICAL-MECHANICAL DERIVATION

Consider an inhomogeneous optical slab with position-dependent index of refraction $n(x)$, as illustrated in Fig. 1. Let the index of refraction vary sufficiently slowly in space so that a density of electromagnetic modes may be defined, at least locally inside the sheet. Now place the optical medium into a region of space that is filled with blackbody radiation in a frequency band $d\omega$ at a temperature $T$. When the electromagnetic radiation inside the medium approaches equilibrium with the external blackbody radiation, the electromagnetic energy density[5] is

$$U = \frac{\hbar\omega}{\exp\left(\frac{\hbar\omega}{kT}\right) - 1} \frac{2d\Omega\, k^2\, dk}{(2\pi)^3}. \tag{1}$$

This is the standard Planck formula for blackbody radiation in a vacuum, but, as Landau and Lifshitz show,[5] it can be adapted to any optical medium by making $k = n\omega/c$. In addition, the energy density may be changed to an intensity $I$ (power per unit area) by multiplying Eq. (1) by the group velocity $v_g = d\omega/dk$. Making both changes in Eq. (1), we obtain:

$$I \equiv U v_g = \frac{\hbar\omega}{\exp\left(\frac{\hbar\omega}{kT}\right) - 1} \frac{2d\Omega\, n^2\, \omega^2}{(2\pi)^3\, c^2}\, d\omega. \tag{2}$$

This differs from the vacuum blackbody intensity simply by the factor $n^2$. Therefore the intensity of light in a medium that is in equilibrium with external blackbody radiation is $n^2$ times greater:

$$I_{\text{int}}(\omega, x) = n^2(\omega, x)\, I_{\text{ext}}^{\text{bb}}(\omega). \tag{3}$$

0030-3941/82/070899-09$01.00 

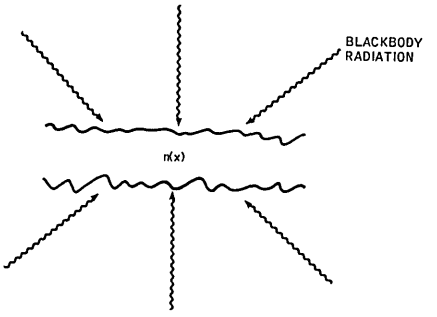


Fig. 1. Textured optical sheet bathed in blackbody radiation. The intensity inside the sheet is greater than that outside by the factor $n^2(x)$.

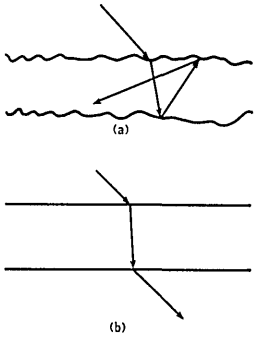


Fig. 2. In the textured sheet (a) the light fills the internal-phase space with radiation of enhanced intensity. In (b) the behavior of the light is nonergodic, and no intensity enhancement occurs.

This factor comes about simply because the density of states in such a medium is proportional to $n^2$, and the equipartition theorem guarantees equal occupation of the states, internal as well as external. This assumes, of course, that the behavior of the light rays internal to the medium is ergodic.

Now let us decide whether, or to what degree, the situation changes when an arbitrary external-radiation field replaces the blackbody radiation. Since we are considering a transparent medium, inelastic events, such as absorption and reemission at another frequency, are not permitted. Therefore each spectral component may be considered individually. In this circumstance, departure of the external field from an exact blackbody frequency distribution will not affect Eq. (3), which will remain valid separately at each frequency $\omega$.

A much more serious question is: What happens when the external-radiation field departs from the isotropic distribution of blackbody radiation? This situation is illustrated in Fig. 2(a), in which the external light is shown to be collimated. If the surface of the optical sheet is quite irregular in shape, then the light rays, on entering the medium, will lose all memory of the external incident angle after the first or, at most, the second scattering from a surface. In other words, all correlation with the external angle will be lost almost immediately on refraction or total internal reflection, especially when averaged over the illuminated surface of the sheet. If this condition is satisfied, then a collimated incident beam of intensity $I_{ext}$ will produce inside the optical sheet a random angular distribution of light, no matter which direction the beam happens to be coming from. Therefore a collimated beam, when it is subdivided so that it illuminates the optical medium equally from all directions, produces identical internal light distributions under those respective conditions. But the condition of isotropic illumination is equivalent to that of blackbody illumination. Therefore Eq. (3) remains valid whether the external field is isotropic, as in the blackbody case, or whether it is collimated, provided again that the light rays internal to the medium behave ergodically:

$$I_{int}(\omega, x) = n^2(\omega, x)\, I_{ext}(\omega). \tag{4}$$

Equation (4) will be corrected for certain surface transmission factors in Section 4, but it is a key formula in this paper. It rests on the assumption that all correlation of the internal rays with the external angle of incidence is lost almost immediately on the rays' entering the medium and/or on their averaging over the illuminated surface. Even optical sheets with ordered surface textures will show the type of randomization that we are discussing here. The reasons are as follows:

1. If light randomization does not occur on the entering refraction, it can occur on the first internal reflection.
2. If it does not occur on the first reflection, then it does on the second.
3. If it does not occur then, it can still be the result of a spatial average over the illuminated surface area.
4. If it does not occur even then, it can still result from angular averaging because of the motion of the source, like the sun moving through the sky.

In other words, there is a rather overwhelming tendency toward randomization in the angular distribution of light and toward the validity of Eq. (4). But it is not always satisfied.

Consider the simple plane-parallel slab shown in Fig. 2(b). Clearly there is no intensity enhancement in that case.[6] Another geometry in which there is no angular randomization is the sphere. The internal angle of incidence is always equal to the internal angle of refraction. There are many other situations in which angular randomization does not occur. These examples show that the key question is whether the optical geometry is ergodic. If it is ergodic, internal angular randomization will tend to occur before the light ray escapes. If it is nonergodic, and angular randomization does not occur, there will be little or no intensity enhancement whether the external radiation is isotropic or not. In Section 3, a semiquantitative criterion is derived to delineate nonergodic geometries from the much larger class of ergodic geometries.

Now consider the situation shown in Fig. (3). In that geometry, the light is confined to a half-space by the presence of a white reflective plane. In effect, the light intensity external to the optical sheet has been doubled by virtue of re-

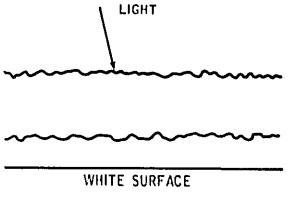


Fig. 3. A white rear reflector reduces the number of escape channels for light by half and therefore increases the internal intensity by a factor of 2.

flection from the white surface. The total intensity enhancement will then be given by

$$I_{\text{int}}(\omega, x) = 2n^2(\omega, x)\, I_{\text{inc}}(\omega), \tag{5}$$

where $I_{\text{inc}}(\omega)$ is the incident-light intensity.

One of the key implicit assumptions that we did not emphasize earlier is that there be no absorption, either within the volume or on the surface of the medium. Optical absorption effects will be treated in Section 5.

Another important assumption is that wave-optical effects can be ignored. Generally, this is a good assumption, as long as the optical sheet is significantly thicker than half of the wavelength of light in the medium. The critical point is that the optical density of modes per unit volume should be relatively unaffected by wave-optical effects. This will be true if the thickness of the optical sheet is much greater than $\lambda/2n$. For a sheet 2 $\mu$m thick, a vacuum wavelength of 1 $\mu$m, and the index of refraction $n = 3.5$ of silicon, this is easily satisfied.

The main conclusion of this section is that a statistical-mechanical approach results in the intensity enhancement given in Eq. (5). The factor $2n^2$ can be quite substantial, i.e., approximately 25 for silicon and approximately 15 for $TiO_2$. Even conventional glass of index 1.5 has an enhancement factor equal to 4.5. In view of the importance of this result, we have given an alternative derivation based on geometrical optics in Section 4.

## 3. ERGODIC BEHAVIOR

We have amply emphasized the importance of ergodic behavior for the results being reported here. A rigorous methematical delineation of those dynamical systems in which phase-space randomization occurs from those in which it does not is difficult. It represents perhaps the major unsolved problem in fundamental statistical mechanics. In this section we merely introduce the subject as it applies to statistical ray optics.

As was mentioned earlier, angular randomization tends to be the rule. On the contrary, it is the nonergodic geometries that are unusual and exceptional. Examples are the plane-parallel slab, the perfect sphere, and the parallelogram. In each of these cases, the symmetry is so high that only a restricted class of angles is dynamically accessible to an incoming light ray. In some respects, the problem has properties similar to the billiard-table problem. A moving billiard ball will access only two discrete angles on a rectangular billiard table. If the billiard table has an odd shape, however, the full angular space is available for the motion.

The problem for photons is somewhat similar, except that (1) it is three-dimensional, and (2) the boundary condition at the edge is not totally reflective, as for billiard balls. When a photon strikes the internal surface of an optical medium it is usually totally internally reflected. But if the internal angle of incidence happens to fall within the escape cone, the light ray can leave the system. The angle of the escape cone $\theta_c$ is defined from Snell's law by the condition for total internal reflection:

$$\sin\theta_c = \frac{1}{n},$$

where $n$ is the index of refraction in the medium.

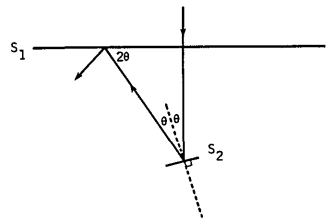


Fig. 4. The angular texturing required at the rear surface to prevent escape on the second bounce at the front surface is relatively small. This may be regarded as a rough guide to the degree of texturing required to ensure that randomization will compete effectively with the escape of light rays through the loss cone.

Therefore optical systems are never completely closed, in contradistinction to billiard tables. The tendency toward angular randomization must compete with escape of the light from the optical medium. Not only must there be randomization but it must come quickly, within one or two refraction or reflection interactions with the surface. Especially for high-index materials, such as semiconductors, this is easily achieved. The solid angle $\Omega_c$ subtended by the escape cone tends to be a rather small fraction of $4\pi$. In fact,

$$\Omega_c \approx \frac{1}{2n^2} \times 4\pi.$$

If we relate solid angle to probability, then the probability for the light's escaping in a single-scattering event is only $1/2n^2$, or about 4% for the index of refraction of silicon. Therefore many surface-scattering events are available for angular randomization before escape becomes probable.

A semiquantitative estimate of the degree for roughness required to satisfy the condition of angular randomization can be made. Consider the optical sheet shown in Fig. 4.

The front surface $S_1$ is flat, whereas the rear surface is roughened. A small portion $S_2$ of the rear surface, whose surface angle departs from normal incidence by $\theta$, is shown. The rear surface is either silvered or backed up by a white reflector. Therefore we consider the possible escape of light rays only from the front surface $S_1$. The critical angle for escape is

$$2\theta = \arcsin(1/n). \tag{6}$$

In other words, the angle of the rear reflector must depart from normal incidence by $\theta > \frac{1}{2}\arcsin(1/n)$ to ensure total internal reflection at the front surface. It should be emphasized that the presence of a quarter-wave antireflection coating will have no effect on the net angle of total internal reflection at the front surface. Substituting the index of refraction 3.5 appropriate to $c$-Si, we find that the angle $\theta$ should be greater than 8.3° to ensure total internal reflection on the second bounce and probable angular randomization on subsequent reflections.

That the angle $\theta$ need only be greater than 8.3° is an indication of the very *mild* degree of surface roughness that is adequate for angular randomization. However, it is only a crude indicator, and it is really applicable only to the geometry of Fig. 4. In the absence of any better approach, $\frac{1}{2}\arcsin(1/n)$ may be regarded as a semiquantitative estimate of the degree of surface roughness required for ergodic behavior.

In Section 4 we show how the intensity-enhancement factor can be more simply derived from geometrical optics rather than from phase-space considerations.

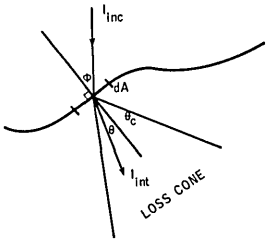


Fig. 5. Detailed balancing requires that the light escaping in the loss cone through area element d$A$ equal the amount of incoming light through the same area element d$A$.

## 4. GEOMETRICAL-OPTICS DERIVATION

Our approach is based on detailed balancing of the light that is incident upon a small area element d$A$ and the light in the loss cone that escapes from it. Consider the geometry shown in Fig. 5. Let $I_{inc}$ be the incident-radiation power per area element d$A$. A fraction $T_{inc}(\phi)$ of this light will be transmitted through the incoming interface, where $\phi$ is the angle of incidence. This must be balanced by the internal radiation that escapes. Let us assume that the internal radiation is isotropic because of the randomizing influence of refraction and reflection from the textured interfaces, as was discussed in the previous section. Let $B_{int}$ be the internal intensity per unit internal solid angle. The internal intensity $I_{int}$ on both sides of an area element d$A$ is given by

$$I_{int} = \int B_{int} \cos\theta \, d\omega,$$

where $\cos\theta$ is the reduction of intensity on the area element due to oblique incidence. In this paper we follow the convention that internal intensity $I_{int}$ is bidirectional while the incident intensity $I_{inc}$ is unidirectional. Therefore

$$I_{int} = 2 \times 2\pi \int_0^{\pi/2} B_{int} \cos\theta \sin\theta \, d\theta,$$

$$I_{int} = 2\pi B_{int}.$$

Only a small fraction of this power per unit area will escape, since the loss-cone solid angle is much less than $4\pi$ sr. The intensity that escapes is

$$I_{esc} = 2\pi \int_0^{\theta_c} \frac{I_{int}}{2\pi} T_{esc}(\theta) \cos\theta \sin\theta \, d\theta, \tag{7}$$

where $n \sin\theta_c = 1$ and $\theta$ is the internal angle of incidence. If we substitute a weighted-average transmission factor $\overline{T}_{esc}$ for the angle-dependent surface transmission factor $T_{esc}(\theta)$, then the integral in Eq. (7) may be easily computed:

$$I_{esc} = I_{int} \frac{\overline{T}_{esc}}{2n^2}.$$

If we now apply the principle of detailed balancing, the entering intensity is made equal to the escaping intensity:

$$T_{inc}(\phi) I_{inc} = I_{int} \times \frac{\overline{T}_{esc}}{2n^2}.$$

Therefore

$$I_{int} = 2n^2 \times \frac{T_{inc}(\phi)}{\overline{T}_{esc}} \times I_{inc}. \tag{8}$$

As Eq. (8) shows, the enhancement may be increased beyond $2n^2$ if $T_{inc}(\phi)$, the transmission factor into the medium, is greater than $\overline{T}_{esc}$, the average transmission factor out of the medium. Of course, time-reversal invariance guarantees that $T_{inc}(\phi) = T_{esc}(\theta)$. If the incident radiation is isotropic, then the ratio $\overline{T}_{inc}/\overline{T}_{esc} = 1$ would appear in Eq. (7), ensuring that the enhancement factor is $2n^2$, as it must be for blackbody radiation. For collimated radiation, an additional small enhancement $T_{inc}(\phi)/\overline{T}_{esc}$ is possible, but this comes at the expense of angular selectivity. This is fully consistent with the ordinary brightness theorem of geometrical optics,[7] which states that intensity increases must come at the expense of angular selectivity. Because of the tendencies toward angular averaging described in Section 2, the factor $T_{inc}(\phi)/\overline{T}_{esc}$ will be approximated as unity, and for most purposes Eq. (8) can be rewritten as

$$I_{int} = 2n^2 \times I_{inc}. \tag{9}$$

It is interesting that Eq. (9) itself could also have been derived directly from the[7] brightness theorem by taking note of the fact that the brightness defined in a medium differs from that in vacuum simply by the factor $n^2$.

The calculation that we have just made is a specific example of an approach that is particularly suited to statistical ray optics. This approach is described by the following three steps:

1. Assume internal angular randomization.
2. Balance inflow and outflow.
3. Integrate over surface and volume.

With these three steps we can solve for intensity enhancement in almost any geometry. This method is particularly suited for dealing with peculiarly shaped media illuminated by collimated light. The enhancement factor can differ significantly from $2n^2$ in that case. The area of the collimated beam that is intercepted may be a strong function of the orientation of the optical medium relative to the oncoming light. This problem does not arise for isotropic illumination, nor does it arise for an optical sheet in which the intensity of an oncoming collimated beam is normalized relative to the frontal area of the sheet.

The intensity increases discussed so far in this paper do not necessarily translate directly into absorption enhancements. This will be the subject of the following section.

## 5. ABSORPTION ENHANCEMENT

Two types of absorption can modify the results that we have presented thus far: volume absorption in the textured optical sheet and surface absorption. In general, both types may be expected to be present. For example, in a semiconductor solar-cell material, there would be absorption in the semiconductor itself and also at the surfaces because of absorption in the transparent electrodes and because of the imperfect reflectors at the rear surface. In this section we model the intensity-enhancement effects allowing for absorption. First we set up a general method. Then we model specific geometries that might be of interest for solar cells.

The approach is as indicated earlier, to balance the input of light from external sources with the loss of light from the optical medium by absorption and refraction through the escape cone. The light input is $A_{inc} I_{inc} T_{inc}$, where $A_{inc}$ is the surface area upon which light is incident and the other sym-

bols have the same meaning as before. To estimate the loss of light, we will proceed along the same lines as in Section 6. We will assume that the light internal to the medium is isotropic because of the randomizing influence of refraction and reflection. There will be three contributions to light that is lost:

1. Light will escape through the escape cone at the rate

$$\frac{A_{esc} I_{int} \overline{T}_{esc}}{2n^2},$$

where $A_{esc}$ is the surface area from which light can escape, which is not necessarily equal to $A_{inc}$, and the other symbols have the same meaning as before.

2. Light may be absorbed because of imperfect reflection from the boundaries:

$$\int_0^{\pi/2} \eta A_{refl} I_{int} \cos\theta \sin\theta \, d\theta = \frac{\eta A_{refl} I_{int}}{2},$$

where $\eta$ is the fractional absorption that is due to imperfect reflection at the boundaries and $A_{refl}$ is the surface area of imperfect reflection.

3. Finally there may be absorption within the bulk:

$$\int \alpha \frac{I_{int}}{2\pi} dV d\Omega = \alpha l I_{int} A_{inc} \int_0^{\pi} \sin\theta \, d\theta = 2\alpha l I_{int} A_{inc}, \tag{10}$$

where $dV$ is a volume element in the bulk, $\alpha$ is the absorption coefficient, and Eq. (10) may be regarded as a definition of the effective thickness $l$. This will be approximately the mean thickness of the sheet. Equation (10) implicitly assumes that the bulk absorption is sufficiently weak that $I_{int}$ is uniform throughout the volume.

Equating the light gained to the light lost,

$$A_{inc} T_{inc} I_{inc} = \left( \frac{A_{esc} \overline{T}_{esc}}{2n^2} + \frac{\eta A_{refl}}{2} + 2\alpha l A_{inc} \right) I_{int}. \tag{11}$$

Regarding $I_{int}$ as the unknown, the expression may be rewritten:

$$I_{inc} = \frac{T_{inc} I_{inc}}{\left( \frac{A_{esc}}{A_{inc}} \frac{\overline{T}_{esc}}{2n^2} + \frac{\eta A_{refl}}{2A_{inc}} + 2\alpha l \right)}. \tag{12}$$

Although Eq. (12) is much more complex than Eqs. (7) and (8), there are many realistic situations in which the simpler expressions are adequate approximations.

One of the main questions that we have is the extent to which the effects that we have been discussing will act to enhance volume absorption. By using Eq. (12), the volume absorption may be written as

$$2\alpha l A_{inc} I_{int} = \frac{2\alpha l A_{inc} T_{inc} I_{inc}}{\left( \frac{A_{esc}}{A_{inc}} \frac{\overline{T}_{esc}}{2n^2} + \frac{\eta A_{refl}}{2A_{inc}} + 2\alpha l \right)}.$$

The fraction of the incoming light that is absorbed in the volume is

$$f_{vol} \equiv \frac{2\alpha l A_{inc} I_{int}}{A_{inc} I_{inc}} = \frac{2\alpha l T_{inc}}{\left( \frac{A_{esc}}{A_{inc}} \frac{\overline{T}_{esc}}{2n^2} + \frac{\eta A_{refl}}{2A_{inc}} + 2\alpha l \right)}. \tag{13}$$

This reduces simply to the transmission factor $T_{inc}$ of the incoming light in the limit of the high absorption coefficient $\alpha$.

A corresponding expression may be written for the total fraction absorbed, including absorption that is due to imperfect reflection at the surfaces:

$$f_{tot} = \frac{2\alpha l + \frac{\eta A_{refl}}{2A_{inc}}}{\left( \frac{A_{esc}}{A_{inc}} \frac{\overline{T}_{esc}}{2n^2} + \frac{\eta A_{refl}}{2A_{inc}} + 2\alpha l \right)} T_{inc}. \tag{14}$$

The absorption enhancement in Eqs. (13) and (14) is of direct interest for weakly absorbing indirect-gap semiconductors, such as crystalline silicon. As Eq. (13) shows, volume absorption can be substantial even when $\alpha l$ is only $1/4n^2$, which is $1/50$ for silicon. The use of these formulas is best illustrated by some specific examples, which are given in Sections 7 and 8.

In Section 6 we treat a new type of antireflection coating that works on the basis of angular randomization and total internal reflection.

## 6. ANTIREFLECTION COATINGS

There are several optical principles on which antireflection coatings are based. The most famous is the quarter-wave coating, which employs destructive interference to reduce the reflectivity of a surface almost to zero. These can be effective, albeit only at a specific wavelength.

Sometimes simple index matching is used. In such cases, a surface coating subdivides one large index-of-refraction discontinuity into two smaller index steps. If the coating is thick, the reflection from the two interfaces is incoherent, unlike the quarter-wave case. Then the reflectivity is simply the sum of the individual reflectivities from the two interfaces. The sum is invariably less than the reflectivity of the original uncoated surface. Although the reduction in reflectivity is modest, at least it is independent of wavelength in this case.

The type of antireflection coating that we will discuss here is a modification of the incoherent index-matching approach. We will find that the effectiveness of the surface coating can be greatly enhanced by texturing and light trapping. The enhancement factor of antireflection behavior is similar to the *intensity enhancement* we have discussed until now.

Consider the geometry shown in the insert in Fig. 6. A layer of polymethyl methacrylate (PMMA) is sprayed onto a textured-silicon surface. We are concerned primarily with those visible and infrared wavelengths that are fully absorbed by the silicon. The incident light experiences a transmission factor $T_{inc}$ at the front surface of the plastic. Since the silicon is assumed to be absorbing, the transmission factor at the plastic–silicon interface may be regarded as the absorption factor $\eta$ for the rear surface of the plastic. At that point in the problem, the reflected light $(1 - \eta)$ is randomized in direction, and Eq. (14) can be used to describe the total absorption of the reflected fraction $(1 - \eta)$. Since the plastic is transparent, $\alpha l$ drops out of Eq. (14). In addition, all the areas are the same: $A_{inc} = A_{esc} = A_{refl}$. The total absorption is the sum of $T_{inc}\eta$, the absorption before randomization plus the fraction of the reflected light $T_{inc}(1 - \eta)$ that is absorbed:

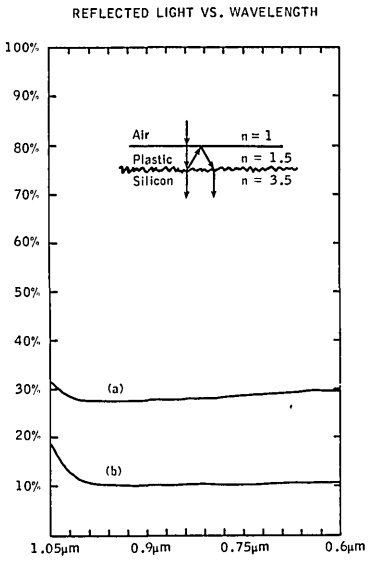


Fig. 6. A thin plastic film on a textured silicon surface combines an index match with light trapping to produce a superior antireflection coating [curve (*b*)]. Texturing alone, without the plastic layer, produces only ~ 2% reduction in surface reflectivity [curve (a)].

$$\text{Absorption} = T_{\text{inc}}\,\eta + T_{\text{inc}}(1-\eta)\frac{\eta}{\dfrac{\overline{T}_{\text{esc}}}{n^2}+\eta}, \qquad (15)$$

where the second part of Eq. (15) is the simplified form of Eq. (14). The formula may be rewritten in the following form:

$$\text{Absorption} = T_{\text{inc}}\frac{\eta}{1-(1-\eta)\Big/\left(1+\dfrac{\overline{T}_{\text{esc}}}{n^2}\right)}. \qquad (16)$$

There is another approach toward calculating the absorption; that is, to calculate the fractional absorption on each reflection and sum reflections to obtain the total absorption in a geometric series. This gives rise to a similar formula:

$$\text{Absorption} = T_{\text{inc}}\frac{\eta}{1-(1-\eta)\left(1-\dfrac{\overline{T}_{\text{esc}}}{n^2}\right)}. \qquad (17)$$

In the limit of large $n^2$ equations, Eqs. (16) and (17) are the same. For index $n = 1.5$ for the plastic and 3.5 for the silicon, $\eta = 0.84$ and $T_{\text{inc}} = 0.96$. We can approximate the angle-averaged escape-transmission $\overline{T}_{\text{esc}}$ factor to be equal to $T_{\text{inc}}$ the incident-transmission factor. With these parameter values, the absorption in Eq. (17) is 89%, whereas the absorption in Eq. (16) differs from this value by about 2%. Therefore the reflection should be reduced to ~11%.

The type of antireflection that we are discussing here should be distinguished from the graded-index effect that texturing would produce on a bare silicon surface. Curve (a) of Fig. 6 shows the reflectivity observed in an integrating sphere for the bare roughened surface. The reflectivity drops slightly from 31%, the polished surface value, to ≈29% for the textured surface. Therefore texturing alone had very little effect in this case. Neither should this type of antireflection coating be confused with the simple index-matching mechanism, which would give a reflectivity of ≈20%. The antireflection coating that we have been describing combines synergistically both the index matching and the texturing to take advantage of a new mechanism, namely, light trapping by total internal reflection in the thin plastic film. According to Eq. (17), the reflectivity should be reduced to 11%. From curve (b) of Fig. 6, we see that the reflectivity indeed drops to 11%. The good agreement is surprising since the index of the plastic film is only 1.5 and Eq. (6) requires a considerably larger texturing angle for randomization than would be required for silicon.

The reflectivity of 11% should not be compared to a best-possible reflectivity of 0%. Solar cells are almost always encapsulated behind glass for practical reasons. Therefore the lowest possible value is 4% because of the reflectivity of the top glass surface. Thus we should be regarded as having achieved a reflectivity within 11% − 4% = 7% of the best possible value.

In this section we have considered light trapping in a thin plastic film on a textured-silicon wafer. In Section 7 we consider the trapping of light inside the wafer itself.

## 7. LIGHT TRAPPING IN TEXTURED-SILICON WAFERS

In the past decade, there have been a number of suggestions for the use of light trapping by total internal reflection to increase the effective absorption in the indirect-gap semiconductor, crystalline silicon. The original suggestions[1,2] were motivated by the prospect of increasing the response speed of silicon photodiodes while maintaining high quantum efficiency in the near infrared.

Subsequently, it was suggested[3] that light trapping would have important benefits for solar cells as well. High efficiency could be maintained while the thickness of semiconductor material required was reduced. Additionally, the constraints on the quality of the silicon could be relaxed since the diffusion length of minority carriers could be reduced proportionately to the degree of intensity enhancement. With such important advantages, interest in this approach has continued, but progress in this field has been hindered because there was no method available to calculate the degree of enhancement to be expected.

For example, St. John[1] mentions that total internal reflection will result in two or more passes of the light rays with a proportionate intensity enhancement. On the other hand, Redfield[3] regards the number of light passes, or degree of enhancement, as an adjustable parameter that could vary anywhere between 1 and 100, and he plots the collection efficiency as a function of this parameter. In calculating the ideal efficiency of silicon solar cells, Loferski *et al.*[4] seemed to imply that perfect light trapping might be possible, which corresponds to an infinite degree of enhancement.

With the methods and logic of statistical ray optics, we now know that we can expect to enhance the absorption by a factor $4n^2$. This has the effect of improving the utilization of those weakly absorbed infrared photons near the band edge by that ratio. The absorption-enhancement factor is twice the intensity-enhancement factor because of angle-averaging effects.

Some experiments were done to confirm these effects by measuring the backscattered light from a wafer in an integrating sphere. The geometry was as shown in Fig. 7. [Curve (a) in Fig. 6 was measured in a similar geometry, except that the rough side of the wafer was facing the integrating sphere.]

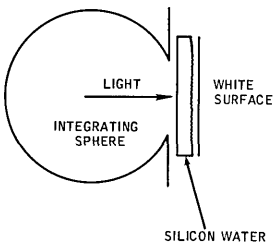


Fig. 7. Geometry used to measure absorption enhancement in a silicon wafer, textured in the rear.

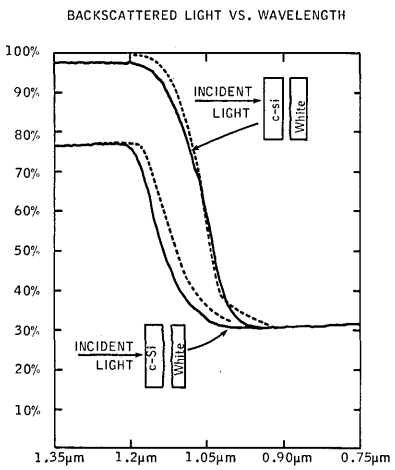


Fig. 8. Comparison of the light absorption in a plane-parallel slab with a textured sheet. The two experimental configurations are almost identical, but the results are quite different. The effective position of the band edge is shifted to the infrared in the light-trapping case. The dashed lines are the theory given by Eq. (14) for the statistical case and by a simple double pass absorption formula in the nonergodic case.

As before, the philosophy of the integrating-sphere measurement is that the fractional absorption in the sample is one minus the observed reflectivity.

In Fig. 7, the polished side of the wafer faces the integrating sphere. The main idea is to compare the overall reflectivity when the rear surface is either ground rough or polished smooth. The comparison is made in Fig. 8. With both faces polished, we have a plane-parallel plate, the situation described in Fig. 2(b), where angular randomization within the silicon does not occur. The light simply makes a round trip in the wafer.

On the other hand, if the rear surface of the silicon is ground rough, internal angular randomization does occur. We may apply Eqs. (13) and (14) to this situation. The Fresnel transmission of the silicon front surface $T_{\text{inc}}$ is about 0.68. The areas $A_{\text{esc}}$ and $A_{\text{inc}}$ are the same and are equal to the front surface area. The rear surface was covered with $MgCO_3$, an almost perfect white reflector, which is frequently used as a reference of whiteness. In the geometry of Fig. 7, the edges of the silicon wafer are actually external to the integrating sphere. Some of the internally trapped light therefore escapes across the cylindrical surface defined by the periphery of the round opening in the integrating sphere. This cylindrical surface in the silicon can be regarded as an imperfect reflector of area $A_{\text{refl}} = 2\pi rl$, where $r$ is the radius of the opening in the integrating sphere. Therefore

$$A_{\text{refl}}/A_{\text{inc}} = 2\pi rl/\pi r^2 = 2l/r.$$

The parameters in this experiment were $r = 1$ cm and $l = 0.025$ cm. The quantity $\eta$, which represents the departure from unit reflectivity at this edge, is difficult to estimate *a priori*, since it depends on the details of the roughness. The value $\eta = 0.82$ describes well the wavelength-independent backscattered light in Fig. 8 in the transparent region between 1.2 and 1.35 $\mu$m. With these values of parameters and the known[8] wavelength-dependent absorption coefficient, a fairly good fit is obtained between $(1 - f_{\text{tot}})$ from Eq. (14) and experiment through the band-edge-transition wavelengths (dashed and solid lines, respectively, in Fig. 8).

The geometry described in Figs. 7 and 8 is a favorable one for solar cells and was first described[1,2] some time ago. Figure 8 shows clearly the shift of the effective absorption edge toward the infrared for the light-trapping case.

## 8. GRANULAR SILICON SHEETS

Another geometry that has received some interest[9] consists of grains of silicon embedded in a sheet of transparent binder, as shown in Fig. 9. It has already been recognized that the light that falls in the transparent plastic between the grains is not wasted. It tends to be trapped and eventually finds its way into the silicon grains. We may analyze that situation in a similar way as previously. Let us denote the quantities pertaining to the incident light by the subscript 1, those pertaining to the silicon by the subscript 2, and those pertaining to the plastic by the subscript 3. Let us also assume that the white backing layer is perfectly reflective. In accordance with the recipe given at the end of Section 4, the energy balance for the plastic may be written as

$$\frac{A_{23}\,\overline{T}_{23}\,I_2}{2(n_2/n_3)^2} + A_{13}\,T_{13}\,I_1 = \left(\frac{A_{13}\,\overline{T}_{13}}{2n_3{}^2} + \frac{A_{23}\,\overline{T}_{23}}{2}\right) I_3, \quad (18)$$

where the first expression on the left-hand side is the light escaping from the silicon into the plastic and the second expression is the incident light. On the right-hand side are the two terms describing the escape of light into the air and into the silicon, respectively. A similar energy balance may be written for the silicon:

$$\frac{A_{23}\,\overline{T}_{23}\,I_3}{2} + A_{12}\,T_{12}\,I_1 = \left(\frac{A_{12}\,\overline{T}_{12}}{2n_2{}^2} + \frac{A_{23}\,\overline{T}_{23}}{2(n_2/n_3)^3} + 2\alpha l\,A_{12}\right) I_2. \quad (19)$$

Here, there is an additional term because of absorption, and $l$ represents a typical absorption thickness of the silicon grain. Equations (18) and (19) should be regarded as two simultaneous equations in the two unknowns $I_2$ and $I_3$. A specific numerical solution would be helpful in estimating the extent to which light falling between the grains tends to be wasted. For this purpose, let us assume that the area of the sheet oc-

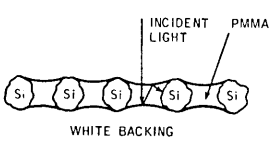


Fig. 9. Monolayer sheet of silicon granules embedded in plastic on a white filter paper. Light is trapped both in the silicon and the plastic binder, resulting in favorable conditions for light collection in a solar cell.

cupied by the silicon grains $A_{12}$ equals the area $A_{13}$ filled in by the plastic. For numerical simplicity, let us assume also that $A_{23}$ is also the same area. For the indices of refraction, take $n_2 = 3.53$ in the silicon and $n_3 = 1.5$ in the plastic. For the transmission factor $\overline{T}_{23}$ of the plastic–silicon interface, take the normal-incidence Fresnel reflectivity, $1 - (n_2 - n_3)^2/(n_2 + n_3)^2 = 0.84$. Let us assume that there is an antireflection coating for the incident rays into the silicon so that $T_{12} \approx 0.96$, which is the same as the transmission coefficient into the plastic. With these values of parameters, the simultaneous Eqs. (18) and (19) can be solved:

$$I_2 = \left(\frac{0.8316}{\alpha l + 0.0319}\right) 0.96 I_1, \tag{20}$$

where $0.96I_1$ is the transmitted incident intensity, and the quantity in parentheses is a type of enhancement factor. The important implications of Eq. (20) become apparent only on examination of its various limits. Consider, for example, the situation in the region of wavelengths within the bandgap of silicon where $\alpha = 0$. Then

$$I_2 = \frac{0.8316 \times 0.96}{0.0319} I_1,$$

which just happens to be $25I_1$ or $2n_2^2 I_1$. This, of course, must be according to the considerations of Section 2.

The most important parameter that we are interested in is the absorption in the silicon. This may be expressed as

$$2\alpha l I_2 = \frac{1.6632\alpha l}{0.0319 + \alpha l} \times 0.96 I_1, \tag{21}$$

when normalized to the area of the silicon grains.

In the limit of small $\alpha l$, the enhancement factor is $4n_2^2$, as expected for absorption. In the limit of large $\alpha l$, i.e., in the visible-wavelength range for silicon,

$$\lim_{\alpha \to \infty} 2\alpha l I_2 = 1.66632 \times 0.96 I_1. \tag{22}$$

According to Eq. (22), the power absorbed by the silicon exceeds the power actually falling on the silicon by a factor of 1.6632. This is because the silicon collects not only those rays that it intercepts directly but also a major fraction of those intercepted by the plastic. Since only a fraction of the incident light will tend to escape the plastic, the balance (≈0.66) will tend to be collected by the adjacent silicon grains. In other words, 83% of the light that enters the sheet will end up being used, in spite of the fact that the area coverage of the silicon grains is only 50%. If the surface-area ratios were more favorable than the conservative assumptions in this calculation, then an even greater fraction of the light would end up in the silicon. The extraordinary utility of the structure described in Fig. 9 is doubly confirmed when it is also realized that, because of the enhancement in the low-absorption regime, the thickness of the layer of grains can be reduced by 50. Therefore, all the advantages of a thin solar cell mentioned at the beginning of Section 7 would accrue to the structure in Fig. 9, not the least of which is the likelihood of that structure's being cheaper to fabricate than conventional silicon solar cells.

The mathematical methods described in this section are meant to suggest the approach that can be used for intensity enhancement in the presence of absorption. Refinements are still needed for the high-absorption case. The formulas given here tend to underestimate the absorption in that instance since they assume randomization. But the absorption may be complete before randomization sets in.

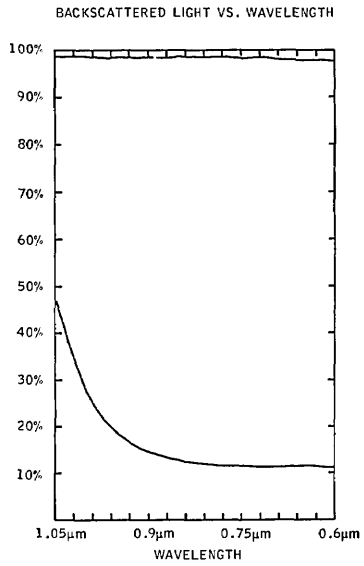


Fig. 10. Reflectivity of the structure shown in Fig. 9. The absorption was ~ 89%, in spite of an area coverage of less than 60%. In addition, band-edge absorption is greatly enhanced. The upper curve shows that the reflectivity of the plastic-covered paper is near 99% in the absence of the silicon grains.

To confirm the quantitative predictions for the optical properties of granular sheets, the structure of Fig. 9 was fabricated in our laboratory. Silicon granules of 99.999% purity were passed through a wire mesh to select a very uniform size distribution averaging 40 $\mu$m in diameter. The grains were placed in a monolayer on a white filter paper. They were then sprayed with a solution of PMMA in toluene. After the solvent evaporated, the plastic bound the particles to the filter paper. The transparent binder also filled in the spaces between the silicon grains. Approximately 50–60% of the area was covered by the grains with the intervening spaces filled in by the binder. Therefore the structure bore a close resemblance to Fig. 9. The reflectivity of the structure was measured in an integrating sphere as before and plotted in Fig. 10. Since the thickness of the layer of grains was very small (approximately equal to the grain diameter), no corrections for the light escaping around the edges were necessary. Therefore Fig. 10 may be directly interpreted in terms of the absorption being one minus the reflectivity.

Two important observations stand out in Fig. 10. The absorption at those wavelengths where the silicon is opaque greatly exceeds the area coverage of silicon, i.e., the absorption percentage is 89%, whereas the silicon coverage was certainly less than 60%. This confirms the prediction of Eq. (22). This performance is quite gratifying, especially insofar as no special antireflection coating is required. In addition, the effective band edge for absorption is shifted toward the infrared compared with a planar silicon sheet with the same mean thickness of the silicon, averaged over the total area, of less than 25 $\mu$m, i.e., the $4n^2$ enhancement factor ensures that we will collect those weakly absorbed infrared rays just as we did in Fig. 8. The dashed lines in Fig. 10 are the theory according to Eq.

(21). Thus we confirm the extraordinary benefits of the structure described in Fig. 9 for solar-cell applications.

In this paper we have shown the utility of a statistical-mechanical approach toward the ray optics of textured and inhomogeneous sheets. This work was motivated mainly by its applicablity toward solar cells and other types of solar collectors. The basic enhancement factor for intensity of $2n^2$ becomes $4n^2$ for bulk absorption, and $n^2$ for surface absorption, because of angle averaging effects. Because many semiconductors tend to have large indices of refraction $n$, these effects are particularly important in those materials.

## ACKNOWLEDGMENT

I would like to thank R. M. Swanson for pointing out an error in the original manuscript.

## REFERENCES

1. A. E. St. John, "Multiple internal reflection structure in a silicon detector which is obtained by sandblasting," U.S. Patent No. 3,487,223 (1969).
2. O. Krumpholz and S. Maslowski, "Schnelle Photodioden mit wellenlangenunabhangigen Demodulatonseigenschaften," Z. Angew. Phys. **25,** 156 (1968).
3. D. Redfield, "Multiple-pass thin-film silicon solar cell," Appl. Phys. Lett. **25,** 647 (1974).
4. M. Spitzer, J. Shewchun, E. S. Vera, and J. J. Loferski, "Ultra-high efficiency thin silicon *p-n* junction solar cells using reflective surfaces," in *Proceedings of the Fourteenth IEEE Photovoltaic Specialists Conference* (Institute of Electrical and Electronics Engineers, New York, 1980), p. 375.
5. L. D. Landau and E. M. Lifshitz, *Electrodynamics of Continuous Media* (Pergamon, New York, 1969).
6. Another situation in which Eq. (4) is not valid is an optically thick turbid sheet illuminated from only one side. In this case, angular averaging is no problem, but spatial averaging will be incomplete. The side of the sheet away from the source of illumination will be dark.
7. M. Born and E. Wolf, *Principles of Optics* (Macmillan, New York, 1964).
8. M. Neuberger and S. J. Welles, *Silicon* (National Technical Information Service, Springfield, Va., 1969), p. 113.
9. J. S. Kilby, J. W. Lathrop and W. A. Porter, "Light energy conversion," U.S. Patent No. 4,136,436 (1979); T. S. T. Velde "Electrical monograin layers and method for making same," U.S. Patent No. 3,625,688 (1971).